Available online at www.sciencedirect.com
ScienceDirect
Tetrahedron
Tetrahedron 63 (2007) 9195–9205

Synthesis, electrochemical, and photophysical studies of multicomponent systems based on porphyrin and ruthenium(II) polypyridine complexes

Xien Liu,[a] Jianhui Liu,[a,*] Jingxi Pan,[a] Samir Andersson[b] and Licheng Sun[a,b,*]

[a]*State Key Laboratory of Fine Chemicals, Dalian University of Technology, Zhongshan Road 158-46, Dalian 116012, PR China*
[b]*School of Chemical Science and Engineering, Department of Chemistry, Royal Institute of Technology (KTH), 10044 Stockholm, Sweden*

Received 25 December 2006; revised 16 June 2007; accepted 19 June 2007
Available online 30 June 2007

Abstract—Two ruthenium tris-bipyridine functionalized porphyrins **4**, **8** and their Zn derivatives **4–Zn**, **8–Zn** were designed, synthesized, and characterized. The redox potentials of these complexes as well as their corresponding monomeric reference porphyrin and ruthenium bipyridine complexes were also measured for comparison. Primary dynamic studies on the electron injection and backing recombination between these complexes and TiO_2 nanoparticles were carried out by means of transient absorption spectroscopy. The results indicate that a long-lived charge separation state was obtained in these assemblies.

1. Introduction

Photoinduced electron transfer or energy transfer processes in supramolecular species (molecular dyads, triads, and tetrads) consisting of metalloporphyrin and ruthenium polypyridine complexes are currently the objective of extensive investigations.[1] Many of these have been based on the excited state chemistry of metalloporphyrin and ruthenium polypyridine and on their favorable electrochemical, photophysical, and photochemical properties.[2] The important reasons for such investigations arise from the interest in mimicking the structures and functions of photosynthesis,[3] construction of the nanometer scale wires,[4] switches,[5] logic gates,[6] and other molecular devices.[7] These functions may be achieved by programming such assemblies through molecule design, so they can transfer energy or electron in one particular direction. This is possible by using binuclear or trinuclear complexes with different metals or by having different terminal ligand substituents. We have a particular interest in the assembly of polychromophore systems, especially those involving metalloporphyrin and ruthenium polypyridine. Recently, we have shown that the intramolecular electron transfer from the higher excited state S_2 of a zinc porphyrin to a covalently linked ruthenium complex was possible.[1e,f,8] Herein, we report the synthesis, electrochemical properties, and photophysical behavior of the bis- and tris-ruthenium tris(bipyridine)-substituted porphyrin complexes, with the reference compounds listed in Figure 1.

2. Results and discussion

2.1. Synthesis

The basic skeleton of our target molecules is a porphyrin connected ruthenium polypyridine complexes at its two or three *meso* positions. The desired molecule **4** was synthesized from the requisite precursor **1** of cis-A_2B_2 type. Porphyrin **1** was prepared according to the known procedure[9] (Scheme 1) and was separated from the other porphyrin products, which include bis(*cis*, *trans*)-, tris- and tetrakis-nitrophenyl-substituted porphyrins. The tris(4-nitrophenyl) porphyrin **5** was obtained in the same batch. The 12% yield for both products should be considered good in giving the two desired porphyrins **1** and **5** simultaneously. Except for porphyrins **1** and **5**, bis(trans) and tetrakis analogs were not collected due mainly to their extremely low yields, although analysis of this mixture by TLC indicated that these isomers could be separated. $SnCl_2$/HCl was used for the subsequent aromatic nitro group reduction[10] to afford the amino derivative **2** in good yield. Hydrochloric acid can also prevent the complexation of tin to free porphyrin. The following amidation with 4′-methyl-2,2′-bipyridinyl-4-carbonyl chloride[11] resulted in the formation of compound **3** in moderate yield. In the following coordination step, 2 equiv of

* Corresponding authors. E-mail: liujh@dlut.edu.cn

0040–4020/$ - see front matter © 2007 Elsevier Ltd. All rights reserved.
doi:10.1016/j.tet.2007.06.074

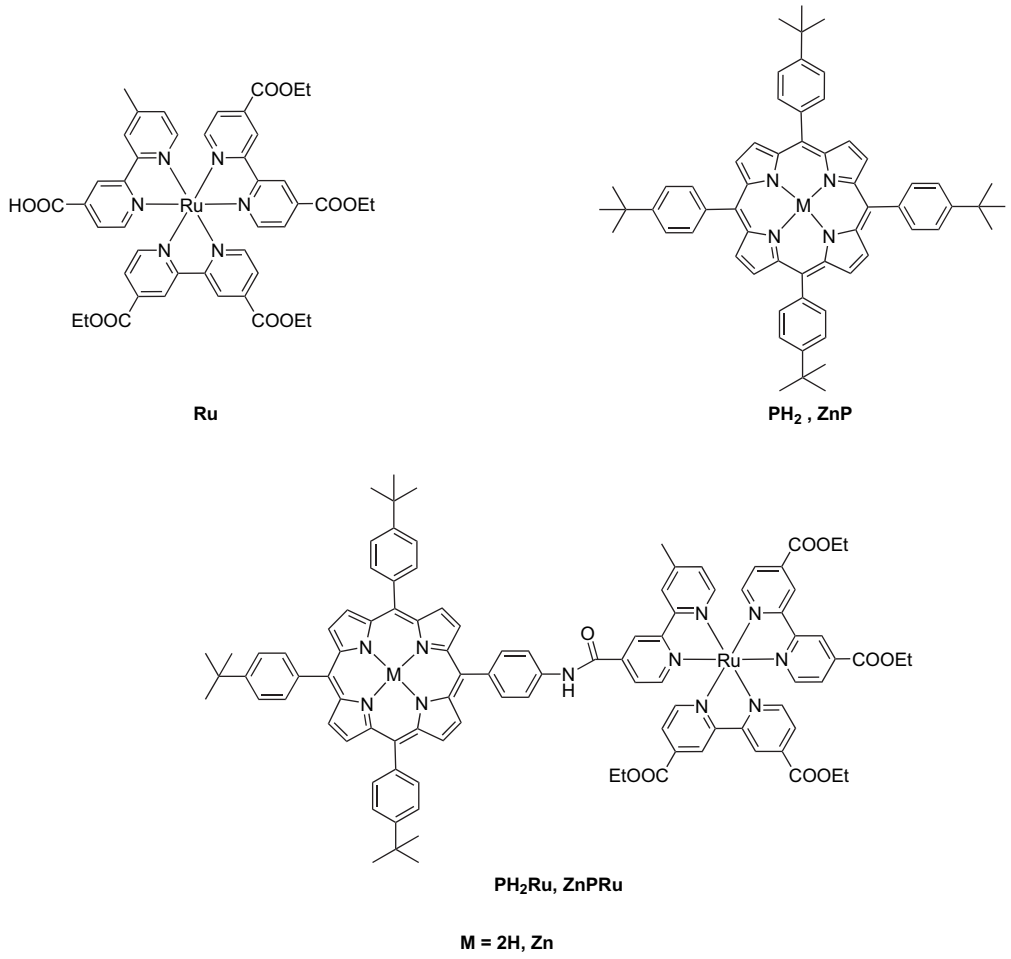

Figure 1. The structures of reference compounds studied.

cis-Ru(4,4′-di-CO_2Et-2,2′-bpy)$_2Cl_2$ was needed for the complete transformation[12] to give the stable ruthenium(II) coordination complex **4** in yield of 35%. Different reaction conditions were examined to improve the yield without any success. The possible reason is either the coordination ability of bipyridine decreases remarkably by the existence of the amide bond or the first ruthenium complex formed will prevent the coordination of the second bipyridine with ruthenium due to the charge repulsion of two Ru(II) ions. Finally, Zn(II) insertion was accomplished with Zn(OAc)$_2$ in chloroform with a little EtOH at room temperature to afford the corresponding Zn(II) porphyrin complex **4**–**Zn** in almost quantitative yield. In a similar manner starting from porphyrin **5**, we also obtained tris-*meso*-ruthenium tris(bipyridine) porphyrin **8** as well as its Zn(II) complex **8**–**Zn** (Scheme 2). All of the compounds were insoluble in hexane or alcohols but were very soluble in most other organic solvents, such as acetonitrile or dichloromethane. Characterization of these complexes has been made by ^{1}H and ^{13}C NMR, mass spectrometry, IR, UV–vis spectroscopy, and elemental analyses. The ^{1}H NMR spectrum of **4** is analyzed as a representative example. It has signals that are consistent with the construction of the amide bond between the porphyrin and the ruthenium tris(bipyridine) subunit at 9.56 ppm. The AA′XX′ spin system of the phenyl protons was identified as a set of dd split occurring between 7.8 and 8.4 ppm. As expected, the β-pyrrolic and porphyrin aromatic protons are located further downfield in the 8.8–9.0 ppm region. The internal NH protons are shielded due to a ring current of the aromatic macrocycle. Thus, the NH of porphyrin **4** containing the ruthenium tris(bipyridine) subunit at the *meso* position resonates at −2.82 ppm, comparable to that of the corresponding smaller-sized substituents porphyrins **2** and **3**, at −2.72 and −2.75 ppm, respectively. This indicates that there was no obvious distortion of the planar macrocyclic structure and therefore a decrease of the ring current effect. More importantly, no diastereoisomers have been discovered through its ^{1}H NMR due to restriction of free rotation between the *meso* carbon and phenyl amide ruthenium tris(bipyridine) subunit. Due to a significant overlap of ^{1}H NMR signals in the aromatic region, combined ^{1}H–^{1}H COSY and TOCSY spectra were taken to assign the protons in the porphyrin complex **4**.

2.2. Electrochemistry

The redox potentials for **4**–**Zn**, **8**–**Zn** and reference compounds **Ru**,[13] **ZnP**,[14] **PH$_2$Ru**,[1e] and **ZnPRu**[1e] (their formulas are listed in Fig. 1) are summarized in Table 1. Reversible electronic waves are observed for the redox processes of all zinc complexes (negative potential range). In addition to the irreversible oxidation peaks at $E_{1/2}$=1.65 (**4**–**Zn**) and 1.62 V

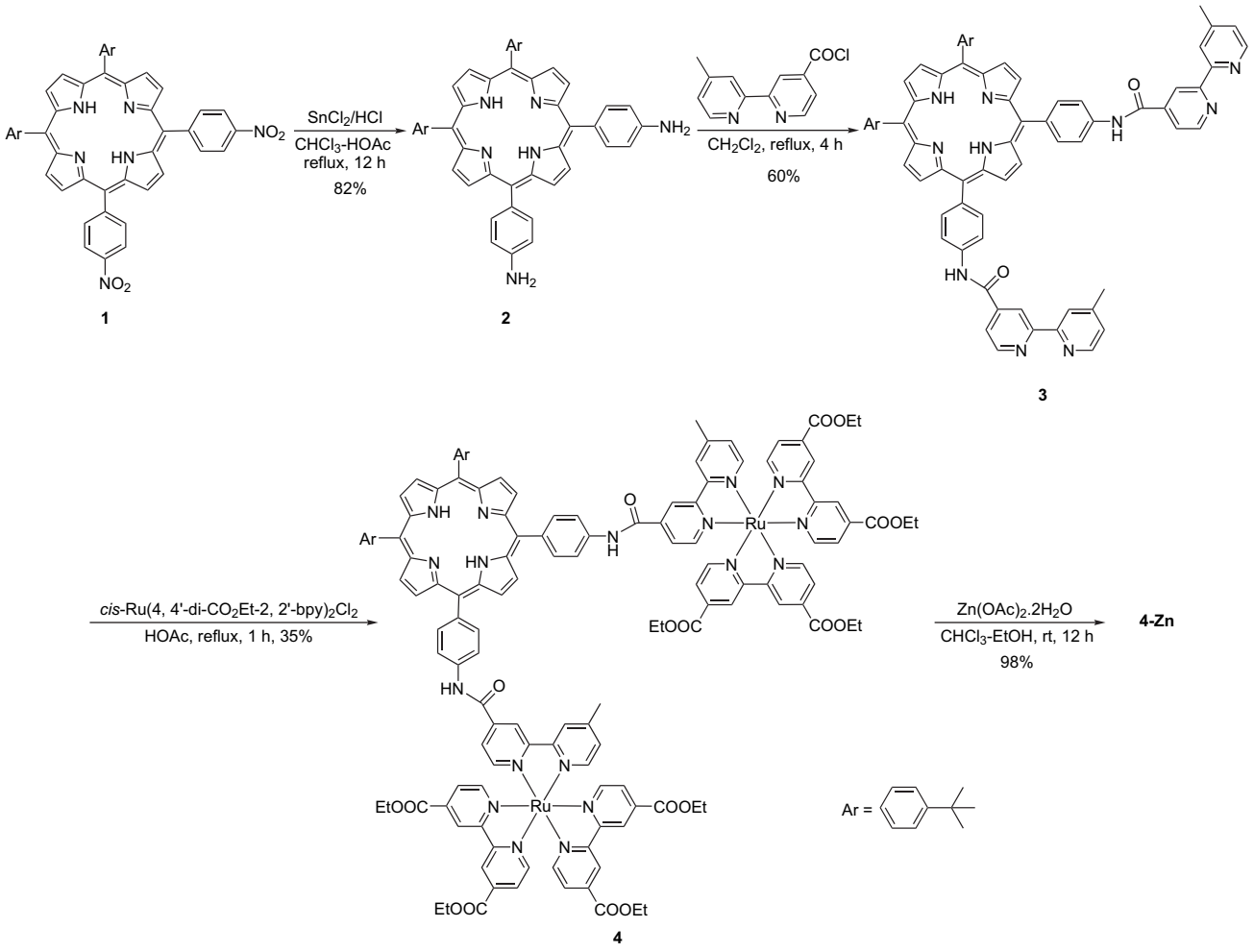

Scheme 1. Synthesis of complex **4**–**Zn**.

(**8**–**Zn**), the complexes **4**–**Zn** and **8**–**Zn** underwent three reversible one-electron reductions and two one-electron oxidations between −1.50 and 2.00 V (see Fig. 2). The reduction for compound **4**–**Zn** occurred at $E_{1/2}$=−0.76, −1.04, and −1.45 V while for **8**–**Zn** at $E_{1/2}$=−0.79, −1.05, and −1.45 V. On the oxidation side, there are two reversible peaks: $E_{1/2}$=0.86 and 1.21 V for **4**–**Zn** and $E_{1/2}$= 0.80 and 1.19 V for **8**–**Zn**. The irreversible peaks were assigned to metal-based oxidation (Ru^{2+}/Ru^{3+}) couple, compared to reference compound **Ru**. The irreversible waves were caused by the introduction of carboxylic groups to the bipyridyl ligands, resulting in different rates of the redox reaction. The different ratio of Ru and porphyrin units was also an important factor. The $E_{1/2}$ values for redox processes of the two zinc complexes are very similar. The different waves could be easily assigned to their individual components by comparison with the redox couples of the reference compounds **Ru** and **ZnP** (see Table 1). These data suggested that the first and second oxidations of the two compounds are related to the ZnP part of the multicomponent while the third oxidation to the Ru subunit. The reductions of them also occurred via stepwise electrode processes involving the bipyridyl ligands and ZnP parts of the multicomponents. On the other hand, the Zn-free counterparts **4**, **8** and their reference compounds **PH_2**,[14] **Ru**, and **PH_2Ru**[1e] (their formulas see Fig. 1) are recorded in Table 2. Different from those in Table 1, we summarized Table 2 according to the oxidation and reduction peaks' order rather than the $E_{1/2}$ values, because these redox processes are mostly irreversible and very intricate, especially at the oxidation side (see complex **4** in Fig. 2). It is evident that the intensity of Ru^{2+}/Ru^{3+} increases with the number of Ru. Energy transfer is favored by the free-base porphyrin. However, the corresponding zinc porphyrin readily underwent oxidative electron transfer.[15] This was the principle reason for the differences observed in redox properties between the free base and zinc complexes.

2.3. Steady-state absorption spectra

The UV–vis absorption spectra of compounds **8** and **8**–**Zn** are shown in Figure 3a. The free-base complex **8** exhibited six distinct absorption maxima in the visible region, and the numerical data of the spectra are summarized in Table 3. Soret bands at around 420 nm ($S_0 \rightarrow S_2$ transition) and Q-bands at 512, 551, 591, and 646 nm ($S_0 \rightarrow S_1$ transition) were observed. UV–vis absorption spectra of the free base **8** in different concentrations are given in Figure 3b. They show that the absorption increases with increasing concentration of free base. In addition, the absorption for the ester-attached $[Ru(bpy)_3]^{2+}$ moiety centered at around 475 nm (MLCT transition) is red shifted by 25 nm relative

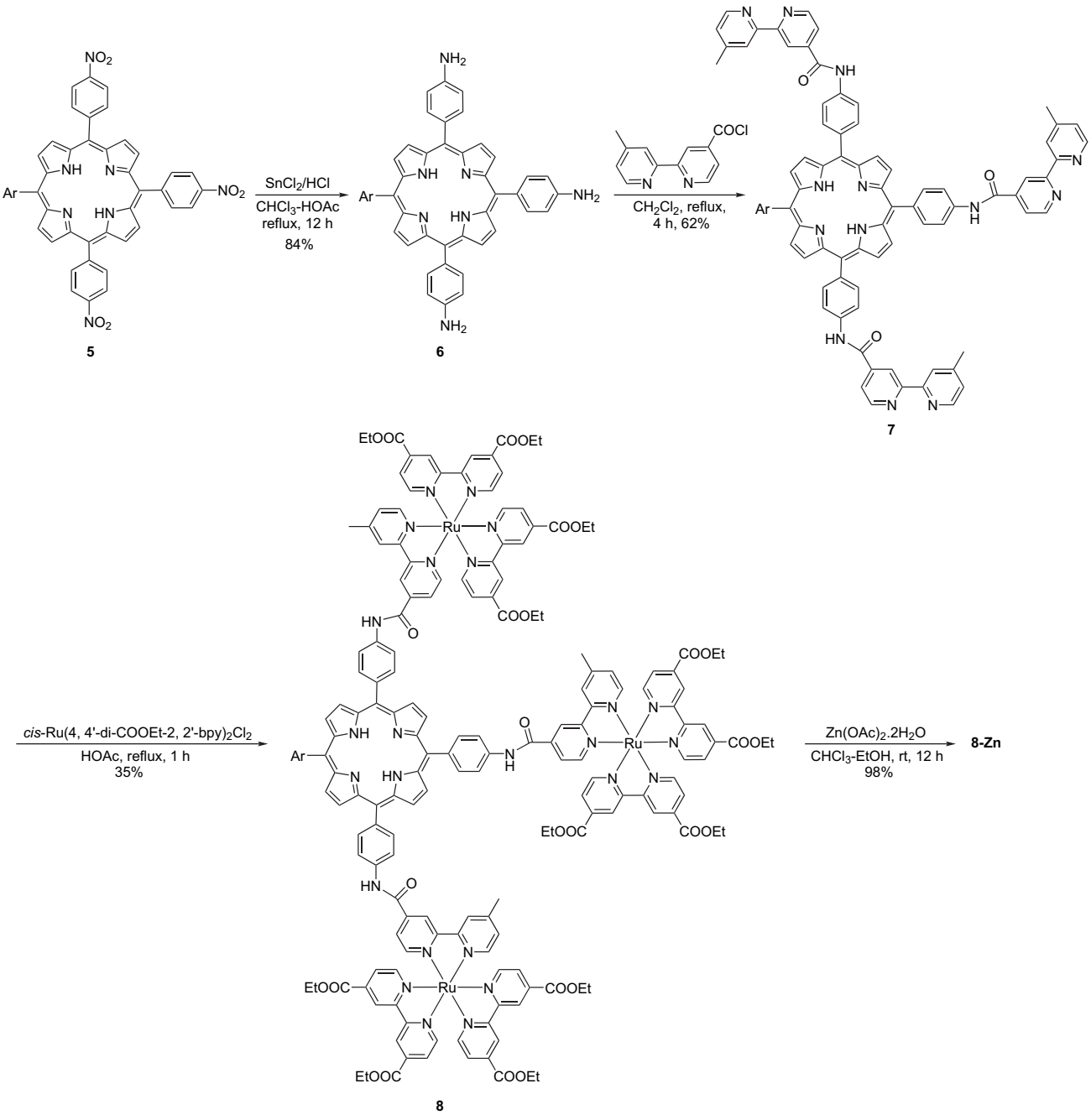

Scheme 2. Synthesis of complex **8**–**Zn**.

to that of the parent $[Ru(bpy)_3]^{2+}$. This effect is attributed to the introduction of ester groups in the pyridine rings.[16] Compound **8**–**Zn** shows two Q-bands due to the increased molecular symmetry of D_{4h}, which is a typical pattern of regular metal porphyrins. The absorption spectra of **4** and **4**–**Zn** are omitted due to their similarity to that of **8** and **8**–**Zn**. The absorption maxima for these complexes are summarized in Tables 3 and 4. Compared to its free base, the maximum absorptions of the Soret band produced a bathochromic shift (10 nm) because of the reduction of the electron density of the porphyrin ring by the insertion of Zn(II). The maximum absorption spectra of Q-bands appeared at 563 and 605 nm as reported previously.[1e]

Table 1. Redox potentials of ZnP based complexes in CH_2Cl_2

	Oxidation $E_{1/2}$ (V vs SCE)				Reduction $E_{1/2}$ (V vs SCE)		
	P/P^+	P^+/P^{2+}	Re/Re^+	Ru^{2+}/Ru^{3+}	L/L^-	L'/L'^-	P/P^-
Ru				1.66	−0.76	−1.02	
ZnP	0.85	1.32					−1.31
ZnPRu	0.78	1.17		1.68	−0.79	−1.07	−1.43
4–**Zn**	0.86	1.21		1.65	−0.76	−1.04	−1.45
8–**Zn**	0.80	1.19		1.62	−0.79	−1.05	−1.45

2.4. Emission measurements

Steady-state fluorescence measurement of **8** and **8**–**Zn** were performed subsequently. Figure 4a shows their fluorescence emission spectra. At room temperature upon excitation of **8**–**Zn** at 552 nm, the only detectable luminescence was

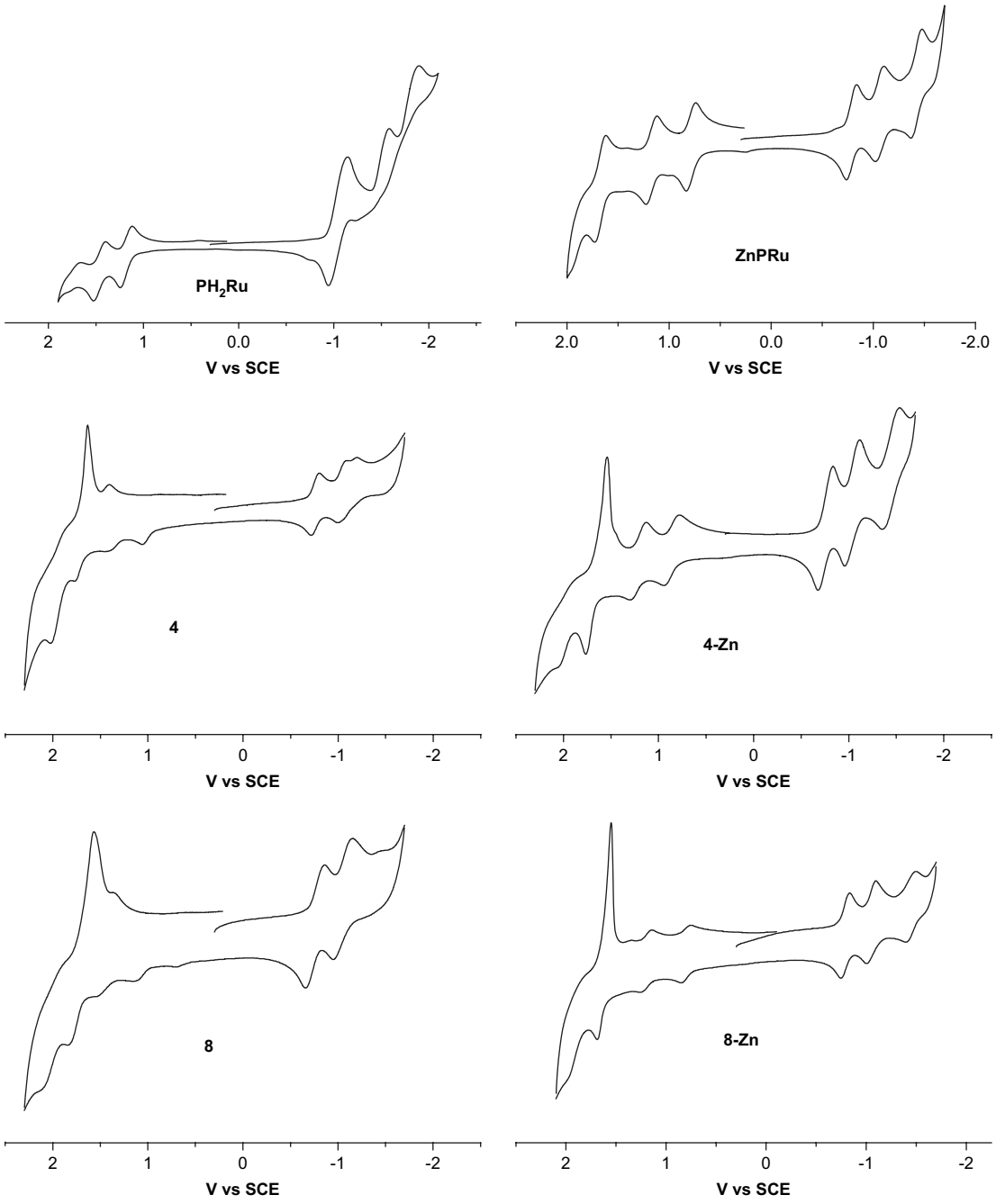

Figure 2. Cyclic voltammogram for complexes **PH_2Ru**, **4**, **8**, **ZnPRu**, **4–Zn**, and **8–Zn** in 10^{-3} M CH_2Cl_2/0.1 M $TBAPF_6$ on a glassy carbon disc electrode at a scan rate of 50 mV/s and reported relative to SCE.

due to the porphyrins, in which the emission from zinc compound was only 2% in intensity relative to that of free-base complex **8**. The very weak emission intensity observed for zinc compounds indicated a strong quenching process, which could be a result of electron transfer from the porphyrin singlet state to the ruthenium moiety. This process is favored by the presence of the heavy metal.[17] On the other hand, the observation of fluorescence only from porphyrins but not from ruthenium moieties indicates that we could excite the zinc porphyrin unit in **8–Zn** selectively, which is crucial for investigating photoinduced electron and energy transfer processes in multicomponent systems. Similarly, **4** and **4–Zn** were faced with the same situation (data not shown). The quantum yields of fluorescence are determined as $\Phi_{f\ \mathbf{4\text{–}Zn}}$=0.00114 and $\Phi_{f\ \mathbf{8\text{–}Zn}}$=0.00065 for **4–Zn** and **8–Zn**, respectively. These values are significantly lower than that of zinc tetraphenylporphyrin (Φ_f=0.031). The numerical data of the spectra are summarized in Tables 3 and 4.

Table 2. Redox potentials of Zn-free porphyrin based complexes in CH_2Cl_2

	Oxidation				Reduction		
	E_{ox}[1]	E_{ox}[2]	E_{ox}[3]	E_{ox}[4]	E_{red}[1]	E_{red}[2]	E_{red}[3]
PH_2	0.62	0.93			−1.45		
Ru			1.54				
PH_2Ru	1.12		1.41		−0.94		
4	1.41		1.63		−0.71		
8	1.35		1.57		−0.66		

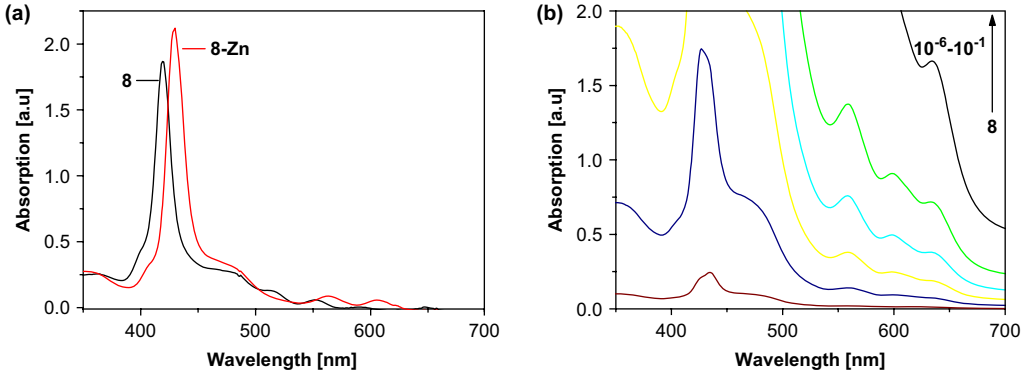

Figure 3. (a) UV–vis absorption spectra of the free base **8** and **8–Zn** in CH_3CN [5×10^{-6}]. (b) UV–vis absorption spectra of the free base **8** in different concentrations [10^{-6}–10^{-1} M].

Table 3. Absorption and emission data of the free bases in acetonitrile solutions at 298 K [5×10^{-6} M]

	Absorption λ_{max} [nm] (ε [M^{-1} cm^{-1}])					Fluorescence λ_{max} [nm] (rt)	
	B (0–0)	Q_y (1–0)	Q_y (0–0)	Q_x (1–0)	Q_x (0–0)	*Q* (0–0)	*Q* (0–1)
4	418 (1.16×10^6)	512 (7.55×10^4)	551 (4.24×10^4)	591 (1.49×10^4)	646 (1.63×10^4)	655	721
8	419 (1.86×10^6)	510 (1.31×10^5)	552 (5.85×10^4)	589 (5.20×10^3)	647 (5.70×10^3)	657	722
PH_2Ru	417 (2.01×10^6)	514 (6.78×10^5)	550 (5.22×10^4)	587 (1.65×10^3)	646 (1.85×10^3)	654	721

Table 4. Absorption and emission data of the zinc complexes in MeCN solutions at 298 K [5×10^{-6} M]

	Absorption λ_{max} [nm] (ε [M^{-1} cm^{-1}])			Fluorescence λ_{max} [nm](rt)	
	B (0–0)	*Q* (1–0)	*Q* (0–0)	*Q* (0–0)	*Q* (0–1)
4–Zn	429 (1.15×10^6)	563 (4.14×10^4)	607 (2.69×10^4)	616	655
8–Zn	430 (2.12×10^6)	563 (8.76×10^4)	605 (5.70×10^4)	618	659
ZnPRu	427 (2.41×10^6)	561 (1.14×10^5)	602 (7.60×10^4)	617	661

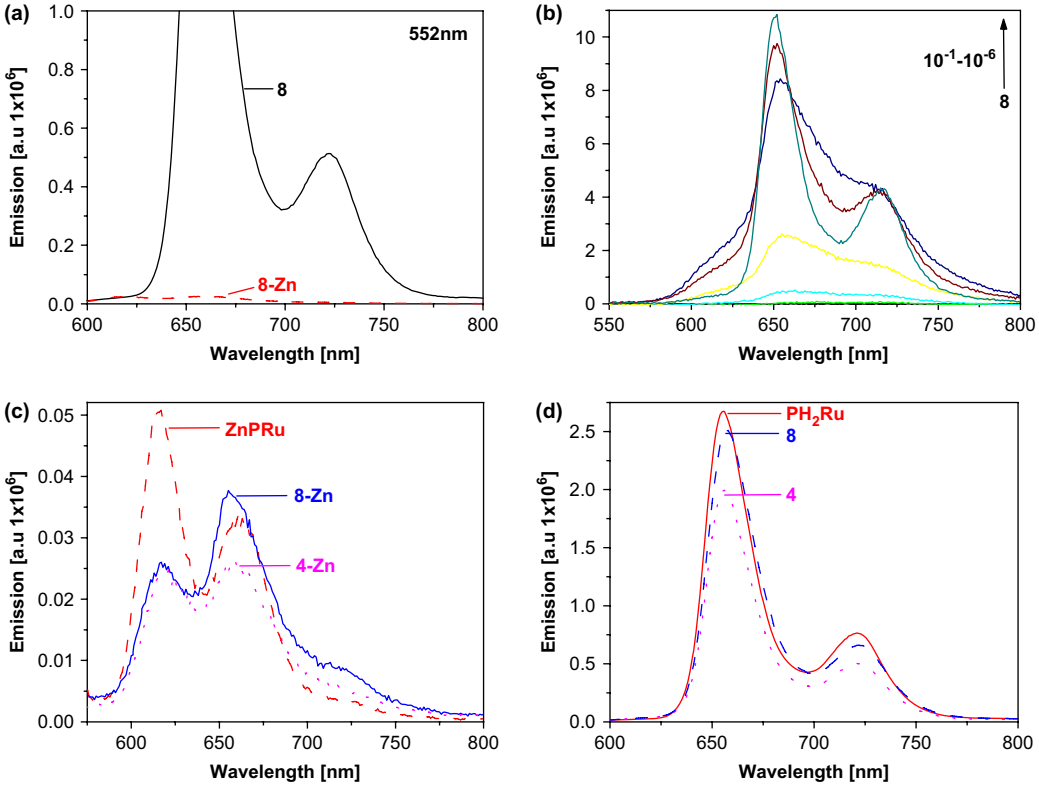

Figure 4. (a) Steady-state emission spectra of **8** and **8–Zn** (λ_{ex}=552 nm) in CH_3CN [5×10^{-6} M]. (b) Steady-state emission spectra of the free base **8** in different concentrations [10^{-1}–10^{-6} M]. (c) Steady-state emission spectra of **4–Zn**, **8–Zn**, and their reference **ZnPRu** (λ_{ex}=552 nm) in CH_3CN [5×10^{-6} M]. (d) Steady-state emission spectra of **4**, **8**, and their reference **PH_2Ru** (λ_{ex}=552 nm) in CH_3CN [5×10^{-6} M].

Figure 4b shows fluorescence emission spectra of the free complex **8** in different concentrations. We could see that its intensity decreased with increased concentration, which indicated that the fluorescence quenching of free complex **8** by intermolecular electron transfer (or energy transfer) became significant at high concentration. Figure 4c and d shows fluorescence emission spectra of **4–Zn**, **8–Zn**, **ZnPRu** and their free-base compounds, respectively, from which we could see that the emission of their porphyrin parts is quenched by introducing Ru units. This is mainly attributed to electron transfer from porphyrin parts to ruthenium units, but the intensity of **8** and **8–Zn** is stronger than that of **4** and **4–Zn**. This result suggests that energy transfer from Ru units to porphyrin parts might occur in these macromolecules. Emission intensity of the compounds **4–Zn**, **8–Zn**, and **ZnPRu** are not proportionate (Fig. 4c), which is different from that of the compounds **4**, **8** and **PH_2Ru** in Figure 4d. This may be caused by trace of free compounds **4** and **8** in **4–Zn** or **8–Zn**, respectively. Further studies of the complicated processes of electron or energy transfer occurring in these systems will be conducted using femtosecond or picosecond transient spectroscopy.

2.5. Time-resolved absorbance

The preliminary transient absorptions and time-dependent decays of **8–Zn** and **8-Zn-TiO_2** have been performed in CH_3CN solution using a YAG laser with a 12 ns pulse width when exciting at 532 nm. Figure 5a shows the spectrum for the triplet absorption of zinc porphyrin unit in **8–Zn** in CH_3CN solution. The $^3(\pi,\pi^*)$ spectrum is marked by an intense absorption at 480 nm and a distinct near-infrared absorption peak, and its kinetic decay exhibits mono-exponential behavior and excited state lifetime is τ=432 ns (Fig. 5c). On the other hand, the transient absorption spectrum of **8-Zn-TiO_2** is quite different from that of **8–Zn** (Fig. 5b). The kinetic decay of **8-Zn-TiO_2** shows di-exponential behavior with lifetimes of charge separation state of τ_1=500 ns and τ_2=15 μs (Fig. 5d). This result indicates a long-lived charge separation obtained in the system, which is very important for mimicking photosynthesis. To investigate the details of the photoinduced electron transfer and energy transfer processes occurring in the complexes **8–Zn** and **8-Zn-TiO_2**, femtosecond transient absorption measurements on this complex are in progress.

In conclusion, we outline in this paper an efficient route toward the preparation of several new multicomponent arrays based on porphyrin and ruthenium polypyridine, including complexes **4**, **8** and their Zn analogues **4–Zn**, **8–Zn**. This is a system that consists of a porphyrin center and one or more ruthenium polypyridine subunits. This kind of structure was designed by considering structural morphology and synthetic strategy. Preliminary investigations of the electronic properties in solution and electrochemical studies clearly revealed that electronic interactions in each subunit are very weak. Steady and transient state spectra recorded at room temperature show that intramolecular

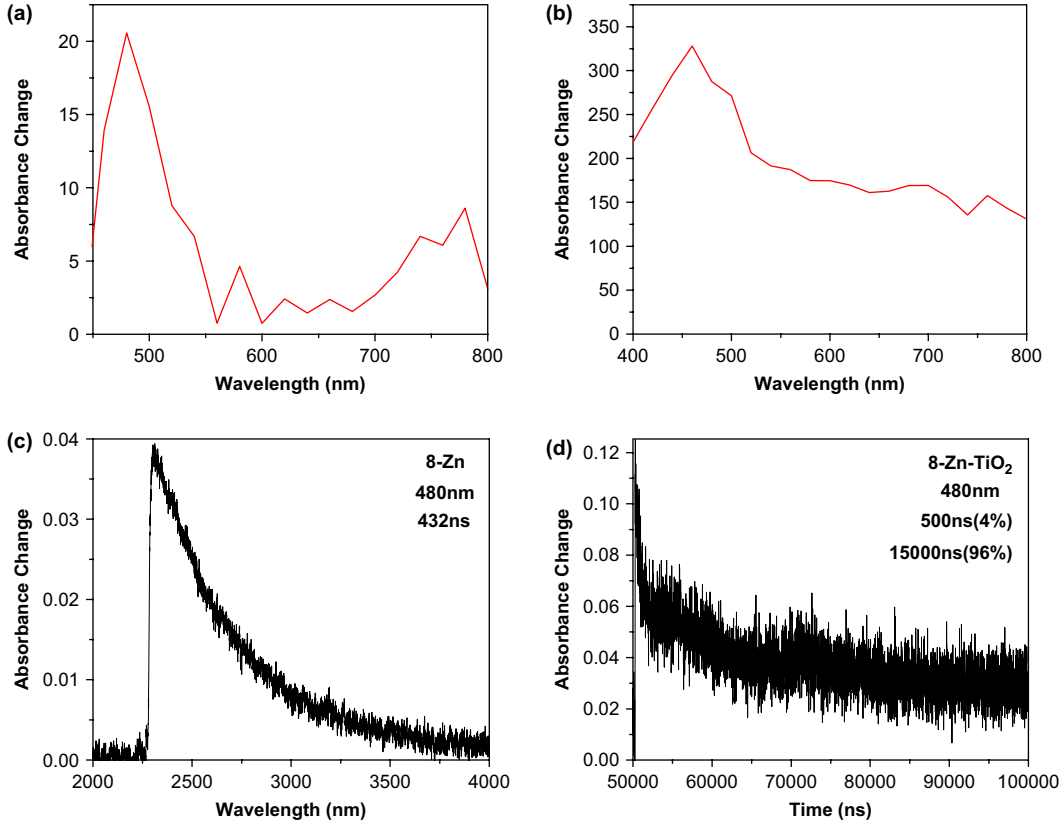

Figure 5. Transient absorption spectrum and time-dependent decay of **8–Zn** and **8-Zn-TiO_2** in deoxygenated CH_3CN solutions (1×10^{-5} M). (a) Transient absorption spectrum of **8–Zn**. (b) Transient absorption spectrum of **8-Zn-TiO_2** (0.5 M $LiClO_4$). (c) Time-dependent decay of **8–Zn** (λ_{probe}=480 nm). (d) Time-dependent decay of **8-Zn-TiO_2** (0.5 M $LiClO_4$) (λ_{probe}=480 nm).

and intermolecular photoinduced electron or energy transfer might occur depending on the concentrations.

3. Experimental

3.1. General

All reagents were purchased from Aldrich, and all solvents were purified according to standard methods. Pyrrole was freshly distilled before use. All of the manipulations were performed under N_2. ^{1}H NMR spectra were recorded on a Varian 400 spectrometer and reported in parts per million downfield from TMS. CH_2Cl_2 (Aldrich, spectroscopic grade) used for performance of electrochemistry was dried with molecular sieve (4 Å) and then freshly distilled from CaH_2 under N_2. Cyclic voltammograms were recorded at a scan rate of 50 mV/s in CH_2Cl_2 solutions (10^{-3} M) using Bu_4NPF_6 (0.05 M) as a supporting electrolyte. Electrochemical measurements were recorded using a BAS-100 W electrochemical potentiostat. The electrolyte solution was degassed by bubbling with dry argon for 10 min before measurements. Cyclic voltammograms were obtained in a three-electrode cell under argon. The working electrode was a glassy carbon disc (diameter 3 mm) successively polished with 3 and 1 μm diamond pastes and sonicated in ion-free water for 10 min. The reference electrode was a non-aqueous Ag/Ag^+ electrode (0.01 M $AgNO_3$ in CH_3CN) and the auxiliary electrode was a platinum wire. The measured potentials in Figure 3 are corrected to the values of SCE by adding 0.30 V. In order to assign easily the protons in the complexes, we showed the numbering scheme of the complex **4** in Figure 6.

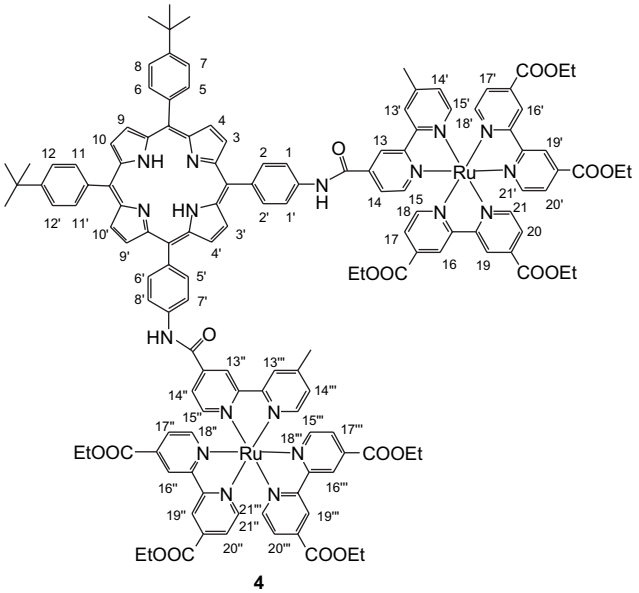

4

Figure 6. The numbering scheme of compound **4** (arbitrary numbering).

3.2. 5,10-Bis(4-nitrophenyl)-15,20-bis(4-*tert*-butylphenyl)porphyrin (1) and 5,10,15-tris(4-nitrophenyl)-20-(4-*tert*-butylphenyl)porphyrin (5)

Pyrrole (0.56 mL, 8.0 mmol), 4-nitrobenzaldehyde (306 mg, 2.0 mmol), and 4-*tert*-butylbenzaldehyde (1.04 mL, 6.0 mmol) were added to CH_2Cl_2 (1000 mL), which was degassed with N_2 for 30 min. After the mixture was stirred and purged with N_2 for a further 30 min, a $BF_3\cdot Et_2O$ solution (1.0 mL, 2 M in CH_2Cl_2, 2.0 mmol) was added dropwise. The reaction mixture was stirred overnight at room temperature. 2,3-Dichloro-5,6-dicyanobenzoquinone (DDQ) (1.82 g, 8.0 mmol) was added to the red-brown solution, and the resulting black mixture was refluxed for 2 h. Et_3N (1.12 mL, 8.0 mmol) was added to the mixture, and the solution was concentrated to dryness under reduced pressure. The residue was purified by column chromatography (silica gel, hexane/CH_2Cl_2 50:50) to give the two desired porphyrin products. Porphyrin **1**: 196 mg, 12%, mp>300 °C; ^{1}H NMR ($CDCl_3$) δ −2.78 (br s, 2H, –NH), 1.61 (s, 18H, *tert*-butyl–H), 7.78 (d, J=8.0 Hz, 4H, H_7, H_8, H_{12}, $H_{12'}$), 8.14 (d, J=8.0 Hz, 4H, H_5, H_6, H_{11}, $H_{11'}$), 8.40 (d, J=8.0 Hz, 4H, H_1, $H_{1'}$, $H_{7'}$, $H_{8'}$), 8.65 (d, J=8.0 Hz, 4H, H_2, $H_{2'}$, $H_{5'}$, $H_{6'}$), 8.73 (d, J=4.8 Hz, 2H, pyrrolyl H), 8.78 (s, 2H, pyrrolyl H), 8.91 (s, 2H, pyrrolyl H), 8.96 (d, J=4.8 Hz, 2H, pyrrolyl H); ^{13}C NMR ($CDCl_3$) δ 31.9, 35.1, 117.1, 122.1, 123.9, 134.7, 135.3, 138.8, 147.9, 149.2, 151.1; APCI-MS positive: $[M+H]^+$(m/z=817.4). Anal. Calcd for $C_{52}H_{44}N_6O_4\cdot 0.1CH_2Cl_2$: C, 75.81; H, 5.40; N, 10.18. Found: C, 76.00; H, 5.52; N, 10.26.

Porphyrin **5**: 193 mg, 12%, mp>300 °C; ^{1}H NMR ($CDCl_3$) δ −2.80 (br s, 2H, –NH), 1.62 (s, 9H, *tert*-butyl–H), 7.80 (d, J=8.8 Hz, 2H, H_7, H_8), 8.13 (d, J=8.0 Hz, 2H, H_5, H_6), 8.40 (d, J=8.4 Hz, 6H, H_1, $H_{1'}$, $H_{7'}$, $H_{8'}$, H_{12}, $H_{12'}$), 8.66 (d, J=8.8 Hz, 6H, H_2, $H_{2'}$, $H_{5'}$, $H_{6'}$, H_{11}, $H_{11'}$), 8.76 (d, J=4.8 Hz, 2H, H_4, H_9), 8.80 (s, 4H, H_3, $H_{3'}$, H_{10}, $H_{10'}$), 8.98 (d, J=4.8 Hz, 2H, $H_{4'}$, $H_{9'}$); ^{13}C NMR ($CDCl_3$) δ 31.9, 35.1, 113.6, 120.0, 120.6, 123.8, 131.1, 132.8, 134.7, 135.9, 139.5, 146.1, 150.6; APCI-MS positive: $[M+H]^+$(m/z=806.3). Anal. Calcd for $C_{48}H_{35}N_7O_6\cdot 0.5CH_2Cl_2$: C, 68.67; H, 4.28; N, 11.56. Found: C, 68.92; H, 4.61; N, 11.90.

3.3. 5,10-Bis(4-aminophenyl)-15,20-bis(4-*tert*-butylphenyl)porphyrin (2)

To a solution of **1** (408 mg, 0.5 mmol) in 1:2 of $CHCl_3$/HOAc (45 mL) was added a solution of $SnCl_2\cdot 2H_2O$ (915 mg, 4.0 mmol) in concentrated HCl (25 mL). The mixture was vigorously stirred in a preheated oil bath (65–70 °C) for 30 min, refluxed overnight, and then neutralized with ammonia solution (25%) to pH 8–9. Chloroform (100 mL) was added, and the mixture was stirred for 1 h. The organic phase was separated, and the water phase was extracted with $CHCl_3$ (2×100 mL). The combined organic layer was washed one time with dilute ammonia solution, three times with water, and then concentrated to dryness. The residue was purified by column chromatography (silica gel, CH_2Cl_2/CH_3CH_2OH 200:1) to give the desired porphyrin product (301 mg, 80%): mp>300 °C; ^{1}H NMR ($CDCl_3$) δ −2.72 (br s, 2H, –NH), 1.60 (s, 18H, *tert*-butyl–H), 3.98 (br s, 4H, $-NH_2$), 7.03 (d, J=8.4 Hz, 4H, H_5, H_6, H_{11}, $H_{11'}$), 7.74 (d, J=8.0 Hz, 4H, H_7, H_8, H_{12}, $H_{12'}$), 7.99 (d, J=8.0 Hz, 4H, H_2, $H_{2'}$, $H_{5'}$, $H_{6'}$), 8.14 (d, J=8.0 Hz, 4H, H_1, $H_{1'}$, $H_{7'}$, $H_{8'}$), 8.86–8.91 (m, 8H, pyrrolyl H). ^{13}C NMR ($CDCl_3$) δ 31.9, 35.1, 113.6, 120.0, 120.6, 123.8, 131.1, 132.8, 134.7, 135.9, 139.5, 146.1, 150.6; APCI-MS positive: $[M+H]^+$ (m/z=757.5). Anal. Calcd for $C_{52}H_{48}N_6\cdot 0.75CH_3CH_2OH$: C, 81.18; H, 6.69; N, 10.62. Found: C, 81.58; H, 6.83; N, 10.21.

3.4. Porphyrin-(NHCO-bpy)$_2$ (3)

A mixture of 4′-methyl-2,2′-bipyridine-4-carboxylic acid (350 mg, 1.64 mmol) and $SOCl_2$ (20 mL) was refluxed for 2 h. After removing excess of $SOCl_2$ by distillation under reduced pressure, the acid chloride product was obtained and dried in vacuum at 70 °C for 1 h. Then dry CH_2Cl_2 (12 mL) was added and the mixture was stirred for 5 min at 50 °C. The resulting light yellow solution was added dropwise to the CH_2Cl_2 (30 mL) solution of **2** (268 mg, 0.35 mmol) in which two drops of Et_3N was preadded. White smoke was observed in the reaction flask. The mixture was refluxed overnight, and washed with aqueous ammonia solution (5%) and then water. After removing the solvent, the residue was dissolved in $CHCl_3$ (20 mL) and then CH_3CN (200 mL) was added dropwise. Precipitate was formed by slowly evaporating $CHCl_3$ under vacuum. The desired product was obtained after column chromatography on silica gel with a mixture of CH_2Cl_2/MeOH (95:5) as eluent to give purple solid (242 mg, 60%): mp>250 °C; ^{1}H NMR ($CDCl_3$) δ −2.75 (br s, 2H, –NH), 1.58 (s, 18H, *tert*-butyl–H), 2.48 (s, 6H, bpy-CH_3), 7.21 (d, J=4.8 Hz, 2H, $H_{14'}$, $H_{14'''}$), 7.71 (d, J=8.0 Hz, 4H, H_5, H_6, H_{11}, $H_{11'}$), 7.96 (d, J=3.2 Hz, 2H, H_{14}, $H_{14''}$), 8.05 (d, J=8.4 Hz, 4H, H_7, H_8, H_{12}, $H_{12'}$), 8.09 (d, J=8.0 Hz, 4H, H_2, $H_{2'}$, $H_{5'}$, $H_{6'}$), 8.20 (d, J=8.4 Hz, 4H, H_1, $H_{1'}$, $H_{7'}$, $H_{8'}$), 8.34 (s, 2H, $H_{13'}$, $H_{13'''}$), 8.59 (d, J=5.2 Hz, 2H, $H_{15'}$, $H_{15'''}$), 8.68 (s, 2H, amide–H), 8.85–8.86 (m, 8H, pyrrolyl–H), 8.88–8.91 (m, 4H, H_{13}, $H_{13''}$, H_{15}, $H_{15''}$); ^{13}C NMR ($CDCl_3$) δ 21.5, 31.9, 35.1, 117.6, 118.8, 119.2, 120.6, 121.7, 122.3, 122.6, 123.5, 125.7, 131.5, 133.3, 134.6, 135.4, 137.4, 139.2, 143.3, 149.1, 150.6, 155.1, 156.9, 163.6; APCI-MS positive: $[M+H]^+$ (m/z=1149.5). Anal. Calcd for $C_{76}H_{64}N_{10}O_2\cdot 0.4CH_2Cl_2$: C, 77.54; H, 5.52; N, 11.84. Found: C, 77.82; H, 5.74; N, 12.00.

3.5. Porphyrin-{NHCO-bpy-Ru[(bpy)-(COOEt)$_2$]}$_2$[PF$_6$]$_4$ (4)

A mixture of **3** (100 mg, 0.087 mmol) and Ru[bpy-$(COOEt)_2]_2Cl_2$ (134 mg, 0.174 mmol) in acetic acid (10 mL) was refluxed for 1 h under N_2 in the dark. After removing the solvent, the product was purified by chromatography on silica gel with a mixture of CH_2Cl_2/MeOH (20:1) as eluent, and the anion was exchanged with NH_4PF_6. The desired product was obtained as a red-brown solid (95 mg, 35%): mp>250 °C; ^{1}H NMR (CD_3CN) δ −2.82 (br s, 2H, –NH), 1.42–1.47 (m, 24H, –$COOCH_2CH_3$), 1.61 (s, 18H, *tert*-butyl), 2.64 (s, 6H, bpy–CH_3), 4.48–4.52 (m, 16H, –$COOCH_2CH_3$), 7.36 (d, J=5.6 Hz, 2H, $H_{14'}$, $H_{14'''}$), 7.57 (d, J=5.6 Hz, 2H, $H_{15'}$, $H_{15'''}$), 7.85–7.87 (m, 8H, H_7, H_8, H_{12}, $H_{12'}$, H_{14}, H_{15}, $H_{14''}$, $H_{15''}$), 7.93–8.05 (m, 16H, H_{17}, $H_{17'}$, $H_{17''}$, $H_{17'''}$, H_{18}, $H_{18'}$, $H_{18''}$, $H_{18'''}$, H_{20}, $H_{20'}$, $H_{20''}$, $H_{20'''}$, H_{21}, $H_{21'}$, $H_{21''}$, $H_{21'''}$), 8.16 (d, J=8.4 Hz, 4H, H_5, H_6, H_{11}, $H_{11'}$), 8.23 (d, J=8.4 Hz, 4H, H_1, $H_{1'}$, $H_{7'}$, $H_{8'}$), 8.30 (d, J=8.4 Hz, 4H, H_2, $H_{2'}$, $H_{5'}$, $H_{6'}$), 8.69 (s, 2H, $H_{13'}$, $H_{13'''}$), 8.88–8.95 (m, 8H, H_3, $H_{3'}$, H_4, $H_{4'}$, H_9, $H_{9'}$, H_{10}, $H_{10'}$), 9.09–9.13 (m, 10H, H_{13}, $H_{13''}$, H_{16}, $H_{16'}$, $H_{16''}$, $H_{16'''}$, H_{19}, $H_{19'}$, $H_{19''}$, $H_{19'''}$), 9.56 (br s, 2H, amide–H); API-ES-MS m/z: $[M-2PF_6]^{2+}$ 1421.4, $[M-3PF_6]^{3+}$ 899.1, $[M-4PF_6]^{4+}$ 638.0. Anal. Calcd for $C_{140}H_{128}F_{24}N_{18}O_{18}P_4Ru_2\cdot CH_2Cl_2$: C, 52.63; H, 4.07; N, 7.84. Found: C, 52.99; H, 3.89; N, 7.49.

3.6. Zn-porphyrin-{NHCO-bpy-Ru[(bpy)-(COOEt)$_2$]}$_2$[PF$_6$]$_4$ (4–Zn)

A solution of $Zn(OAc)_2\cdot 2H_2O$ (20 mg, 0.100 mmol) in ethanol (2 mL) was added to a solution of **4** (80 mg, 0.025 mmol) in chloroform (15 mL), and stirred at room temperature overnight under N_2 in the dark. This mixture was washed with water, evaporated to dryness, and purified by CH_2Cl_2/MeOH (10:1). The desired product was obtained as a red-brown solid (76 mg, 95%): mp>250 °C; ^{1}H NMR (CD_3CN) δ 1.41–1.46 (m, 24H, –$COOCH_2CH_3$), 1.62 (s, 18H, *tert*-butyl), 2.63 (s, 6H, bpy–CH_3), 4.46–4.52 (m, 8H, –$COOCH_2CH_3$), 7.36 (d, J=6.0 Hz, 2H, $H_{14'}$, $H_{14'''}$), 7.56 (d, J=5.2 Hz, 2H, $H_{15'}$, $H_{15'''}$), 7.82–7.88 (m, 8H, H_7, H_8, H_{12}, $H_{12'}$, H_{14}, H_{15}, $H_{15''}$, $H_{15''}$), 7.93–8.06 (m, 16H, H_{17}, $H_{17'}$, $H_{17''}$, $H_{17'''}$, H_{18}, $H_{18'}$, $H_{18''}$, $H_{18'''}$, H_{20}, $H_{20'}$, $H_{20''}$, $H_{20'''}$, H_{21}, $H_{21'}$, $H_{21''}$, $H_{21'''}$), 8.15 (d, J=8.0 Hz, 4H, H_5, H_6, H_{11}, $H_{11'}$), 8.19 (d, J=8.8 Hz, 4H, H_1, $H_{1'}$, $H_{7'}$, $H_{8'}$), 8.69 (s, 2H, $H_{13'}$), 8.86–8.93 (m, 8H, H_3, $H_{3'}$, H_4, $H_{4'}$, H_9, $H_{9'}$, H_{10}, $H_{10'}$), 9.07–9.13 (m, 10H, H_{13}, $H_{13''}$, H_{16}, $H_{16'}$, $H_{16''}$, $H_{16'''}$, H_{19}, $H_{19'}$, $H_{19''}$, $H_{19'''}$), 9.68 (br s, 2H, amide–H); API-ES-MS m/z: $[M-2PF_6]^{2+}$ 1452.0, $[M-3PF_6]^{3+}$ 921.0, $[M-4PF_6]^{4+}$ 654.0. Anal. Calcd for $C_{140}H_{126}F_{24}N_{18}O_{18}P_4ZnRu_2\cdot 1.2CH_2Cl_2$: C, 51.42; H, 3.92; N, 7.64. Found: C, 51.69; H, 3.67; N, 7.39.

3.7. 5,10,15-Tris(4-aminophenyl)-20-(4-*tert*-butylphenyl)porphyrin (6)

To a solution of **5** (402 mg, 0.5 mmol) in 1:2 of $CHCl_3$/HOAc (45 mL) was added a solution of $SnCl_2\cdot 2H_2O$ (915 mg, 4.0 mmol) in concentrated HCl (25 mL). The mixture was vigorously stirred in a preheated oil bath (65–70 °C) for 30 min, refluxed overnight, and then neutralized with ammonia solution (25%) to pH 8–9. Chloroform (100 mL) was added and the mixture was stirred for 1 h. The organic phase was separated and the water phase was extracted with $CHCl_3$ (2×100 mL). The combined organic layer was washed one time with dilute ammonia solution, three times with water, and then concentrated to dryness. The residue was purified by column chromatography (silica gel, CH_2Cl_2/CH_3CH_2OH 200:1) to give the desired porphyrin product (304 mg, 85%): mp>300 °C; ^{1}H NMR ($CDCl_3$) δ −2.71 (br s, 2H, –NH), 1.61 (s, 9H, *tert*-butyl–H), 3.99 (br s, 6H, –NH_2), 7.04 (d, J=8.4 Hz, 6H, H_2, $H_{2'}$, $H_{5'}$, $H_{6'}$, H_{11}, $H_{11'}$), 7.74 (d, J=8.0 Hz, 2H, H_5, H_6), 7.99 (d, J=8.4 Hz, 6H, H_1, $H_{1'}$, $H_{7'}$, $H_{8'}$, H_{12}, $H_{12'}$), 8.13 (d, J=8.4 Hz, 2H, H_7, H_8), 8.84–8.90 (m, 8H, pyrrolyl–H); ^{13}C NMR ($CDCl_3$) δ 31.9, 35.1, 113.6, 119.5, 120.4, 123.8, 131.2, 132.8, 134.6, 135.9, 140.1, 146.1, 150.5; APCI-MS positive: $[M+H]^+$ (m/z=716.5). Anal. Calcd for $C_{48}H_{41}N\cdot 0.5CH_3CH_2OH$: C, 79.65; H, 6.00; N, 13.27. Found: C, 79.91; H, 6.05; N, 12.88.

3.8. Porphyrin-(NHCO-bpy)$_3$ (7)

A mixture of 4′-methyl-2,2′-bipyridine-4-carboxylic acid (434 mg, 2.03 mmol) and $SOCl_2$ (20 mL) was refluxed for 2 h. After removing excess of $SOCl_2$ by distillation under reduced pressure, the acid chloride was obtained, and dried in vacuum at 70 °C for 1 h. Then dry CH_2Cl_2 (12 mL) was added and the mixture was stirred for 5 min at 50 °C. The resulting light yellow solution was added dropwise to the CH_2Cl_2 (30 mL) solution of **6** (236 mg, 0.33 mmol) in which

two drops of Et_3N was preadded. White smoke was observed in the reaction flask. The mixture was refluxed overnight, washed with 5% of aqueous ammonia solution, and then with water. After removing the solvent, the residue was dissolved in $CHCl_3$ (20 mL) and CH_3CN (200 mL) was added dropwise. Precipitate was formed by slowly evaporating $CHCl_3$ under vacuum. The desired product was obtained after column chromatography on silica gel with a mixture of CH_2Cl_2/MeOH (90:10) as eluent to give purple solid (279 mg, 65%): mp>250 °C; ^{1}H NMR ($CDCl_3$) δ −2.76 (br s, 2H, –NH), 1.56 (s, 9H, *tert*-butyl–H), 2.47 (s, 9H, bpy–CH_3), 7.19–7.21 (m, 3H, $H_{14'}$, $H_{14'''}$, $H_{14''''}$), 7.65 (d, J=7.2 Hz, 2H, H_5, H_6), 7.94–7.96 (m, 3H, H_{14}, $H_{14''}$, $H_{14''''}$), 8.00–8.07 (m, 8H, H_2, $H_{2'}$, $H_{5'}$, $H_{6'}$, H_7, H_8, H_{11}, $H_{11'}$), 8.15 (d, J=7.6 Hz, 2H, H_1, H_{12}), 8.20 (d, J=8.4 Hz, 4H, $H_{1'}$, $H_{7'}$, $H_{8'}$, $H_{12'}$), 8.32–8.33 (m, 3H, $H_{13'}$, $H_{13'''}$, $H_{13''''}$), 8.57–8.59 (m, 3H, $H_{15'}$, $H_{15'''}$, $H_{15''''}$), 8.73 (s, 3H, amide–H), 8.85–8.91 (m, 14H, pyrrole-8H, H_{13}, $H_{13''}$, $H_{13''''}$, H_{15}, $H_{15''}$, $H_{15''''}$); ^{13}C NMR ($CDCl_3$) δ 21.4, 31.8, 34.9, 117.8, 118.8, 119.5, 122.1, 122.5, 123.7, 125.5, 134.5, 135.3, 137.5, 138.9, 143.2, 148.9, 149.0, 150.5, 155.1, 157.2, 164.5; APCI-MS positive: $[M+H]^+$ (m/z= 1304.4). Anal. Calcd for $C_{84}H_{65}N_{13}O_3\cdot 1.5$EtOH: C, 76.07; H, 5.43; N, 13.26. Found: C, 76.09; H, 5.35; N, 13.06.

3.9. Porphyrin-{NHCO-bpy-Ru[(bpy)-(COOEt)$_2$]}$_3$[PF$_6$]$_6$ (8)

A mixture of **7** (100 mg, 0.087 mmol) and Ru[bpy-$(COOEt)_2]_2Cl_2$ (134 mg, 0.174 mmol) in acetic acid (30 mL) was refluxed for 1 h under N_2 in the dark. After removing the solvent, the product was purified by column chromatography on silica gel with a mixture of CH_2Cl_2/MeOH (20:1) as eluent, and the anion was exchanged with NH_4PF_6. The desired product was obtained as a red-brown solid (95 mg, 35%): mp>250 °C; ^{1}H NMR (CD_3CN) δ −2.80 (s, br, 2H, –NH), 1.40–1.44 (m, 36H, –$COOCH_2CH_3$), 1.60 (s, 9H, *tert*-butyl), 2.61 (s, 9H, bpy–CH_3), 4.46–4.49 (m, 24H, –$COOCH_2CH_3$), 7.34 (d, J=5.2 Hz, 3H, $H_{14'}$, $H_{14'''}$, $H_{14''''}$), 7.54–7.58 (m, 3H, $H_{15'}$, $H_{15'''}$, $H_{15''''}$), 7.82–7.87 (m, 8H, H_7, H_8, H_{14}, H_{15}, $H_{14''}$, $H_{15''}$, $H_{14'''}$, $H_{15''''}$), 7.91–8.02 (m, 24H, H_{17}, $H_{17'}$, $H_{17''}$, $H_{17'''}$, $H_{17''''}$, H_{18}, $H_{18'}$, $H_{18''}$, $H_{18'''}$, $H_{18''''}$, $H_{18'''''}$, H_{20}, $H_{20'}$, $H_{20''}$, $H_{20'''}$, $H_{20''''}$, H_{21}, $H_{21'}$, $H_{21''}$, $H_{21'''}$, $H_{21''''}$, $H_{21'''''}$), 8.16 (d, J=7.6 Hz, 2H, H_5, H_6), 8.21 (d, J=8.4 Hz, 6H, H_1, $H_{1'}$, $H_{7'}$, $H_{8'}$, H_{12}, $H_{12'}$), 8.28 (d, J=8.4 Hz, 6H, H_2, $H_{2'}$, $H_{5'}$, $H_{6'}$, H_{11}, $H_{11'}$), 8.66 (s, 3H, $H_{13'}$, $H_{13'''}$, $H_{13''''}$), 8.87–8.94 (m, 8H, pyrrolyl–H), 9.08–9.11 (m, 15H, H_{13}, $H_{13''}$, $H_{13''''}$, H_{16}, $H_{16'}$, $H_{16''}$, $H_{16'''}$, $H_{16''''}$, $H_{16'''''}$, H_{19}, $H_{19'}$, $H_{19''}$, $H_{19'''}$,$H_{19''''}$, $H_{19'''''}$), 9.71(br s, 3H, amide–H); API-ES-MS m/z: $[M-3PF_6]^{3+}$ 1281.2, $[M-4PF_6]^{4+}$ 924.7, $[M-5PF_6]^{5+}$ 710.7, $[M-6PF_6]^{6+}$ 568.6. Anal. Calcd for $C_{180}H_{161}F_{36}N_{25}O_{27}P_6Ru_3$: C, 50.52; H, 3.79; N, 8.18. Found: C, 50.18; H, 3.97; N, 7.82.

3.10. Zn-porphyrin-{NHCO-bpy-Ru[(bpy)-(COOEt)$_2$]}$_3$[PF$_6$]$_6$ (8–Zn)

A solution of $Zn(OAC)_2\cdot 2H_2O$ (20 mg, 0.100 mmol) in ethanol (2 mL) was added to a solution of **8** (61 mg, 0.025 mmol) in chloroform (15 mL), and stirred at room temperature overnight under N_2 in the dark. This mixture was washed with water and then evaporated to dryness and purified by CH_2Cl_2/MeOH (10:1). The desired product was obtained as a red-brown solid (56 mg, 95%): mp>250 °C; ^{1}H NMR (CD_3CN) δ 1.40–1.44 (m, 36H, –$COOCH_2CH_3$), 1.60 (s, 9H, *tert*-butyl), 2.61 (s, 3H, bpy–CH_3), 4.45–4.52 (m, 24H, –$COOCH_2CH_3$), 7.35 (d, J=7.6 Hz, 3H, $H_{14'}$, $H_{14'''}$, $H_{14''''}$), 7.53 (d, J=5.2 Hz, 3H, $H_{15'}$, $H_{15'''}$, $H_{15''''}$), 7.82–8.03 (m, 32H, H_7, H_8, H_{14}, $H_{14''}$, $H_{14'''}$, H_{15}, $H_{15''}$, $H_{15'''}$, H_{17}, $H_{17'}$, $H_{17''}$, $H_{17'''}$, $H_{17''''}$, $H_{17'''''}$, H_{18}, $H_{18'}$, $H_{18''}$, $H_{18'''}$, $H_{18''''}$, $H_{18'''''}$, H_{20}, $H_{20'}$, $H_{20''}$, $H_{20'''}$, $H_{20''''}$, H_{21}, $H_{21'}$, $H_{21''}$, $H_{21'''}$, $H_{21''''}$, $H_{21'''''}$), 8.16 (d, J=7.6 Hz, 2H, H_5, H_6), 8.19 (d, J=8.8 Hz, 6H, H_1, $H_{1'}$, H_7, $H_{7'}$, H_{12}, $H_{12'}$), 8.25 (d, J=8.8 Hz, 6H, H_2, $H_{2'}$, $H_{5'}$, $H_{6'}$, H_{11}, $H_{11'}$), 8.68 (s, 3H, $H_{15'}$, $H_{15'''}$, $H_{15''''}$), 8.86–8.92 (m, 8H, pyrrolyl–H), 9.06–9.12 (m, 15H, H_{13}, $H_{13''}$, $H_{13''''}$, H_{16}, $H_{16'}$, $H_{16''}$, $H_{16'''}$, $H_{16''''}$, H_{19}, $H_{19'}$, $H_{19''}$, $H_{19'''}$, $H_{19''''}$), 9.56 (br s, 3H, amide–H); API-ES-MS m/z: $[M-3PF_6]^{3+}$ 1302.1, $[M-4PF_6]^{4+}$ 940.0, $[M-5PF_6]^{5+}$ 723.0, $[M-6PF_6]^{6+}$ 579.1. Anal. Calcd for $C_{180}H_{159}F_{36}N_{25}O_{27}P_6Ru_3Zn\cdot$EtOH: C, 49.81; H, 3.79; N, 7.98. Found: C, 49.61; H, 3.92; N, 7.61.

Acknowledgements

Financial support of this work from the following sources is gratefully acknowledged: The Swedish Energy Agency and Swedish Research Council (VR), China Natural Science Foundation (Grant 20128005 and 20672017), The Ministry of Science and Technology (MOST) (Grant 2001CCA02500), and The Ministry of Education. The authors thank Ms. Xin-Mei Fu for MS measurements, Dr. Tomas Polivika and Ms. Kun Jin for helpful discussion.

References and notes

1. (a) Collin, J.-P.; Harriman, A.; Heitz, V.; Odobel, F.; Sauvage, J.-P. *Coord. Chem. Rev.* **1996**, *148*, 63–69; (b) Harriman, A.; Hissler, M.; Trompette, O.; Ziessel, R. *J. Am. Chem. Soc.* **1999**, *121*, 2516–2525; (c) Uyeda, H. T.; Zhao, Y.; Wostyn, K.; Asselberghs, I.; Clays, K.; Persoons, A.; Therien, M. J. *J. Am. Chem. Soc.* **2002**, *124*, 13806–13813; (d) Ambroise, A.; Wagner, R. W.; Rao, P. D.; Riggs, J. A.; Hascoat, P.; Diers, J. R.; Seth, J.; Lammi, R. K.; Bocian, D. F.; Holten, D.; Lindsey, J. S. *Chem. Mater.* **2001**, *13*, 1023–1034; (e) Liu, X.; Liu, J.; Jin, K.; Yang, X.; Peng, Q.; Sun, L. *Tetrahedron* **2005**, *61*, 5655–5662; (f) Liu, X.; Liu, J.; Pan, J.; Chen, R.; Na, Y.; Gao, W.; Sun, L. *Tetrahedron* **2006**, *62*, 3674–3680; (g) Sessler, J. L.; Capuano, V. L.; Burrell, A. K. *Inorg. Chim. Acta* **1993**, *204*, 93–101.
2. Jovanovich, H. B. *Photochemistry of Polypyridine and Porphyrin Complexes*; Academic: New York, NY, 1992.
3. (a) *The Reaction Center of Photosynthetic Bacteria*; Michel-Beyerle, M.-E., Ed.; Springer: Berlin, 1995; (b) Barber, J.; Anderson, B. *Nature* **1994**, *371*, 31–34.
4. Sauvage, J.-P.; Collin, J.-P.; Chambron, J.-C.; Guillerez, S.; Coudret, C.; Balzani, V.; Barigelletti, F.; De Cola, L.; Flamigni, L. *Chem. Rev.* **1994**, *94*, 993–1019.
5. Gilat, S. L.; Kawai, S. M.; Lehn, J. M. *Chem.—Eur. J.* **1995**, *1*, 275–284.
6. Wasielewski, M. R.; O'Neil, M. P.; Gosztola, D.; Niemczyk, M. P.; Svec, W. A. *Pure Appl. Chem.* **1992**, *64*, 1319–1325.
7. Holten, D.; Bocian, D. F.; Lindsey, J. S. *Acc. Chem. Res.* **2002**, *35*, 57–69.

8. LeGourriérec, D.; Andersson, M.; Davidsson, J.; Mukhtar, E.; Sun, L.; Hammarström, L. *J. Phys. Chem. A* **1999**, *103*, 557–559.
9. Lindsey, J. S.; Schreiman, I. C.; Hsu, H. C.; Kearney, P. C.; Marguerettaz, A. M. *J. Org. Chem.* **1987**, *52*, 827–836.
10. Hunter, C. A.; Sarson, L. D. *Angew. Chem., Int. Ed. Engl.* **1994**, *33*, 2313–2316.
11. McCafferty, D. G.; Bishop, B. M.; Wall, C. G.; Hughes, S. G.; Mecklenberg, S. L.; Meyer, T. J.; Erickson, B. W. *Tetrahedron* **1995**, *51*, 1093–1106.
12. Kormann, C.; Bahnemann, W.; Hoffmann, R. *J. Phys. Chem.* **1988**, *92*, 5196–5201.
13. Pan, J.; Xu, Y.; Benkö, G.; Feyziyev, Y.; Styring, S.; Sun, L.; Åkermark, B.; Polivka, T.; Sundström, V. *J. Phys. Chem. B* **2004**, *108*, 12904–12910.
14. Adler, A. D.; Longo, F. R.; Finarelli, J. D.; Goldmacher, J.; Assour, J.; Korsakoff, L. *J. Org. Chem.* **1967**, *32*, 476.
15. Benniston, A. C.; Chapman, G. M.; Harriman, A.; Mehrabi, M. *J. Phys. Chem. A* **2004**, *108*, 9026–9036.
16. Wacholtz, W. F.; Auerbach, R. A.; Schmehl, R. H. *Inorg. Chem.* **1986**, *25*, 227–234.
17. Dixon, I. M.; Collin, J. P. *J. Porphyrins Phthalocyanines* **2001**, *5*, 600–607.